Water-soluble amphiphilic gold nanoparticles with structured ligand shells†

Oktay Uzun, Ying Hu, Ayush Verma, Suelin Chen, Andrea Centrone and Francesco Stellacci*

Received (in Cambridge, UK) 28th August 2007, Accepted 1st October 2007
First published as an Advance Article on the web 19th October 2007
DOI: 10.1039/b713143g

Highly water-soluble mixed monolayer protected "rippled" gold nanoparticles were synthesized through a one step reaction with sodium 11-mercaptoundecanesulfonate and octanethiol ligands at various ratios.

Metal nanoparticles are promising candidates for applications that range from electronics,[1] to energy storage,[2] and to biology. In the latter case, *e.g.* in molecular imaging,[3] phototherapy,[4] or drug delivery vehicles,[5] there is a stringent need for nanoparticles that are highly soluble in physiological solutions. Currently, the most common strategy to achieve water-soluble particles is through charge-stabilization,[5] as is the case for citrate-stabilized gold particles.[6] However, these particles cannot be isolated from solution without irreversible aggregation and have solubilities in the micromolar regime, limiting the breadth of their applications. Other strategies include coating nanoparticles with molecules terminated with ethylene glycol moieties,[7] or the use of both biological and non-biological macromolecules and polymers.[8] These valid approaches have the limitation of being based on entropy-rich coatings (sometimes with disperse thickness) whose interaction with biological materials can be difficult to predict and/or engineer. In many cases the addition of hydrophobic molecules in the ligand shell reduces the particles' solubility even at small loading levels, in contrast to what happens in biological molecules. Here we show that it is possible to achieve high water-solubility in monolayer protected gold nanoparticles (NPs) coated with a mixture of hydrophobic and hydrophilic ligand molecules, even when the hydrophobic content is as high as 66%.

Monolayer protected gold NPs[9,10] are supramolecular assemblies of a highly ordered self-assembled monolayer (SAM)[9,11] 'wrapped' around a single metallic core. The ligand shell determines a large part of the particles' properties.[12] Recently we found that when the ligand shell of a nanoparticle is composed of a binary mixture of ligand molecules that would phase separate into randomly-ordered nanometre-sized domains on a flat surface, ribbon-like domains of alternating composition form on the nanoparticle (see cartoon in Fig. 1).[13] This highly-ordered supramolecular structure consisting of phases that are only a few molecules thick has unique effects on the nanoparticles' properties. In fact, the size of these domains is small enough (~0.5 nm) to be comparable to the size of a small molecule; as a consequence the nanoparticles show a non-monotonic dependence of solubility in ethanol on ligand shell composition as well as some resistance to protein non-specific adsorption.[13] To date, our studies have dealt exclusively with water-insoluble particles. Here, we focus on the structure and properties of NPs coated with anionic ligand shells. We show that ribbon-like domains also form in these particles and that uniquely high water-solubility can be achieved.

While it is relatively easy to obtain monolayer-protected NPs soluble in organic solvents, ligand-coated water-soluble particles are more challenging. We focused on ω-terminated ligands with sulfonate groups, because of their known ability to solubilize protein complexes and their reactivity with platelets.[14] Because of their high charge density and extreme hydrophilicity, mercaptodecanesulfonate SAMs behave as molecular sieves that are selectively permeable to inorganic cations.[15] Moreover, water-soluble homoligand gold nanoparticles functionalized with short chain sodium 3-mercaptopropanesulfonate have been reported to be water-soluble.[16] To achieve water-soluble structured particles with shorter hydrophobic and longer hydrophilic molecules in the ligand shell, we focused on sodium 11-mercaptoundecanesulfonate (MUS) and octanethiol (OT). Charged thiolated molecules can form ordered SAMs on flat gold,[13] hence it is plausible that they can phase separate when co-assembled with hydrophobic thiols on gold surfaces (this, we believe, is the precondition needed to obtain ordered striped domains on nanoparticles).[13,17,18]

Monolayer-protected NPs are often synthesized using the Schriffin two phase approach,[19] in which the reaction takes place

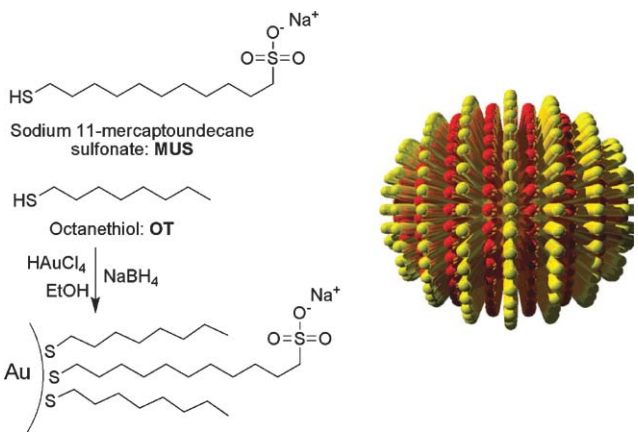

Fig. 1 (*Left*) Schematic of the synthesis of water-soluble nanoparticles with sodium 11-mercaptoundecanesulfonate in the presence of non-polar octanethiol ligands. (*Right*) Cartoon illustrating an idealized nanoparticle coated with a binary mixture of ligands that phase separate into ribbon-like domains of alternating composition. These particles are referred to as 'rippled' throughout the paper.

Department of Materials Science and Engineering, Massachusetts Institute of Technology, Cambridge, MA, USA.
E-mail: frstella@mit.edu; Tel: (+1) 617-452-3704
† Electronic supplementary information (ESI) available: Experimental section, nanoparticle characterization data and ^{1}H NMR spectra. See DOI: 10.1039/b713143g

in a toluene phase. This method has drawbacks when trying to generate water-soluble particles, mostly because of the insolubility of many ligands in toluene. For this reason, we chose a one phase approach.[7] This latter method has the advantage of producing particles whose ligand shell composition typically matches the stoichiometric ratio of ligands used during the synthesis.[20] Briefly, 0.9 mmol of gold salt ($HAuCl_4$) was dissolved in ethanol and 0.9 mmol of the desired thiol mixture was added while stirring the reaction mixture, then a saturated ethanol solution of $NaBH_4$ was added dropwise for 2 h. The solution was stirred for 3 h and the reaction vessel was then placed in a refrigerator overnight. Precipitated particles were collected *via* vacuum filtration with quantitative filter paper. NPs were washed with ethanol, methanol and acetone and dried under vacuum. To completely remove unbound ligands, particles were dialyzed using 5′ segments of cellulose ester dialysis membrane (Pierce, SnakeSkin, MWCO 3500) that were placed in 1 litre beakers of MilliQ water and stirred slowly. The beakers were recharged with fresh water *ca.* every 8 h over the course of 72 h. The NP solutions were collected from the dialysis tubes, and the solvent was removed under vacuum at <45 °C. ^{1}H NMR spectroscopy on the purified particles was performed to determine the absence of unbound ligands (see ESI†). Six different types of nanoparticles were synthesized, varying only in the stoichiometric ratio used during the reaction; in one case only MUS ligands were used, in the other cases we used a 2 : 1, 1 : 1, 1 : 2, 1 : 4, and 1 : 5 MUS to OT ratio, respectively. The ligand shell composition was determined by decomposing the particle core with iodine followed by ^{1}H NMR analysis. The ratios found were, within experimental errors, the same as those of the stoichiometric ratios used. FTIR spectra of these particles showed a high degree of order (*i.e. trans*-planarity) in the ligand molecules.[20] The core size of the particles was characterized using transmission electron microscopy (TEM-JEOL-200 kV). Average core diameters were found to all be in the same range (*e.g.* 4.3 $\pm$ 1.3 nm for all MUS, 4.5 $\pm$ 1.0 nm for MUS : OT 2 : 1, and 4.9 $\pm$ 0.9 nm for MUS : OT 1 : 2).

To determine whether these particles had a structured ligand shell, we imaged them using scanning tunneling microscopy (STM). Our previous studies had focused on water-insoluble particles, hence to image these particles we had to significantly depart from previously used sample preparation methods. Hydrophobic NPs readily adsorb onto gold on mica substrates and are easily imaged in packed monolayers. In the case of strongly hydrophilic particles we only observed individual hydrophilic nanoparticles when samples were prepared in the same manner. In such a case, ligand shell imaging is truly challenging due to tip-induced particle movements. To overcome this problem we had to change sample preparation approaches. Aqueous NP solutions with different concentrations were drop cast onto gold substrates, enclosing the droplet within larger toluene (or benzene) drops and drying under an atmosphere rich in toluene vapor, effectively slowing the drying process and limiting the spreading of the water droplet. An alternative approach was to use water–ethanol mixtures, by first placing an ethanol drop on the center of the substrate and then gently adding a small microlitre drop of an aqueous solution containing the nanoparticles on top of the first drop. The addition of ethanol speeds up the drying process and thus does not allow for a significant concentration of the NPs at the drop edge (*i.e.* the 'coffee stain effect'). The STM imaging parameters used were a set current of 50 pA and a bias voltage between 1 and 1.5 V; imaging speed varied between 0.8 μm s^{-1} and 1.8 μm s^{-1}. All MUS particles showed no feature in the ligand shell despite multiple imaging attempts (not even head groups, probably due to the high hydrophilicity of these particles); while MUS : OT 2 : 1 and 1 : 2 NPs showed the classical striated pattern that we attribute to 'rippled' particles with a spacing of 1.0 $\pm$ 0.2 nm and 1.1 $\pm$ 0.1 nm respectively (Fig. 2). Particles coated with a MUS : OT ratio of 1 : 1 were also found to be 'rippled' but with a narrower spacing of 0.60 $\pm$ 0.1 nm, similar to those found previously on other systems.[13] Particles with a ligand ratio of 1 : 4 and 1 : 5 were mostly insoluble and hence challenging to study with STM, but are not expected to be 'rippled' due to the large imbalance of the two ligand shell components.

Some of the particles synthesized (MUS only, and MUS : OT 2 : 1 and 1 : 2) were found to be highly water-soluble. NP solutions were prepared in both deionized (DI) water and phosphate buffered saline (PBS) at physiological conditions (50 mg/100 μl PBS solution). The solubility of these particles was so high that determining a true saturation concentration was rather difficult. We can state that these particles had a saturation concentration of at least 20% in weight (25 mg in 100 μl) independent of ligand shell composition, that is at that concentration we could not observe any precipitate in the solution even after 1 week. At this concentration the solutions were pitch-black, hence a visual determination of the presence of a precipitate has to be considered only a preliminary measurement. Nevertheless, we believe that particles coated with MUS : OT 2 : 1 were even more soluble than the other two types of particles evaluated (at least 33% in weight). This level of solubility, to the best of our knowledge, is the highest ever reported for gold nanoparticles in any solvent. More importantly it is striking to note that particles coated with as much as 66% of hydrophobic ligands are still remarkably water-soluble. Interestingly, there was no noticeable change in solubility between DI and PBS buffer (pH 7.4). Even at relatively low pH ($\sim$2.3), precipitation was not observed. Using static light scattering measurements, we studied solubility as a function of ionic strength and observed an abrupt transition towards aggregation at a 1 M NaCl concentration. To better characterize the stabilization mechanism of these particles, zeta potentials (ζ, BHI, ZetaPALS instrument) were measured. For pure MUS NPs we measured -45.3 ± 4.4 mV, MUS : OT 2 : 1 and 1 : 2 had ζ of -33.3 ± 6.2 mV and -31.0 ± 3.4 mV respectively in PBS buffer (pH 7.4). The zeta potential does not change upon the addition of more OT molecules. The facts that MUS : OT 2 : 1 is the most water-soluble

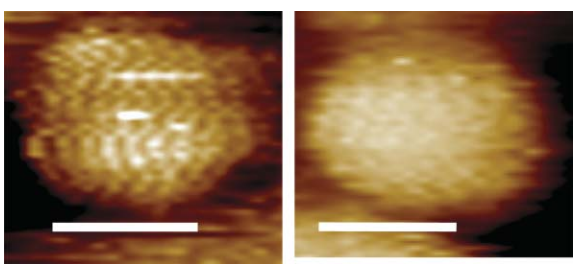

Fig. 2 STM height images of gold NPs coated with a 2 : 1 (*left*) and 1 : 2 (*right*) molar ratio of MUS and OT respectively. The images show the typical striated appearance of 'rippled' NPs of the ones illustrated in the cartoon in Fig. 1. Scale bars are 5 nm.

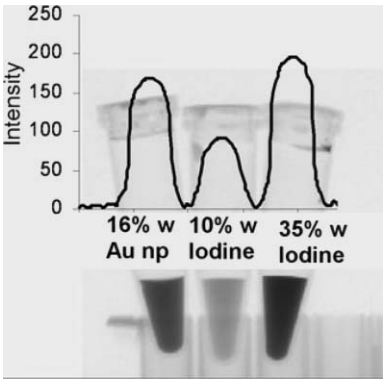

Fig. 3 CT contrast intensity profile and actual CT contrast images.

particle and that ζ does not change as a function of OT concentration could be related to the previously observed non-monotonic dependence of solubility on ligand shell composition, *i.e.* they could be an effect of the ligand shell structure.[13,17]

Not all the particles studied exhibited this remarkable water solubility. MUS : OT 1 : 1 nanoparticles, with narrower ripple structure, were significantly less soluble (<0.5 mg/100 μl) than the other rippled particles. Particles with a large fraction of hydrophobic molecules (and reasonably with no ripple structure) quickly lost their solubility in water. The 1 : 4 MUS : OT particles had a limited water solubility (<0.1 mg/100 μl), and the 1 : 5 were water insoluble. Next, these results were compared to the solubility of particles coated with mixtures of MUA (11-mercaptoundecanoic acid) and OT. We synthesized a range of these particles with composition varying from pure MUA to MUA : OT 1 : 2 using a similar one phase method. We used FTIR to determine that MUA molecules were completely deprotonated at the end of the synthesis. Particles had an average diameter of 4.3 $\pm$ 0.9 nm and are known to have structured (rippled) ligand shells.[13] All of these particles were water-insoluble, with the exception of the homoligand MUA particles (soluble for pH > 4.0).[21] A striking difference is that in these particles a 20% of OT (*i.e.* MUA : OT 4 : 1) completely eliminates water-solubility. It is possible that, in order to rationalize all of these results, space considerations for both the molecules (and hence ligand shell structure) and the counterions have to be taken into account (note that the size of a sulfonate end group is larger than a carboxylate end group). Indeed, mixed ligand MUA particles have been observed to be water-soluble when large counterions are used; in this study we limited ourselves to small counterions.[22]

To better determine the stability of the aqueous solution of concentrated MUS : OT nanoparticles and to investigate a possible application, we used a computerized tomography (CT) scanner to compare the X-ray absorption density with commercial iodinated agents (Fig. 3).[23] 50 mg of MUS : OT 2 : 1 nanoparticles were dissolved in 250 μl physiological buffer, (PBS with 300 mmol NaCl solution). The CT intensity value achieved by 35 wt% of the iodinated contrast agent (190) can be easily achieved by 16 wt% of MUS : OT 2 : 1 nanoparticle solution (170). Importantly there was no precipitation observed by CT imaging over a period of one week in the nanoparticle solution, which is an indication of the stability of these particles in physiological conditions. Finally, these concentrated nanoparticle solutions can successfully be used as an ink and printed by using an HP-thermal inkjet printing system.

In summary, we have shown the synthesis of water-soluble amphiphilic "rippled" nanoparticles. Unprecedented solubility values have been shown even at a high percentage of hydrophobic molecules. The application of these water-soluble NPs to molecular imaging and their cellular-uptake behavior is currently underway.

This research was supported by the NIH TPEN Program and by the NSF CAREER and the Packard Foundation Award. We are grateful to R. Weissleder for allowing us to obtain CT scan images and P. Mardilovich for the help with inkjet printing.

Notes and references

1 C. B. Murray, C. R. Kagan and M. G. Bawendi, *Annu. Rev. Mater. Sci.*, 2000, **30**, 545–610.
2 A. N. Shipway and I. Willner, *Chem. Commun.*, 2001, 2035–2045.
3 I. H. El-Sayed, X. H. Huang and M. A. El-Sayed, *Nano Lett.*, 2005, **5**, 829–834.
4 C. Loo, A. Lowery, N. Halas, J. West and R. Drezek, *Nano Lett.*, 2005, **5**, 709–711.
5 G. Han, C. C. You, B. J. Kim, R. S. Turingan, N. S. Forbes, C. T. Martin and V. M. Rotello, *Angew. Chem., Int. Ed.*, 2006, **45**, 3165–3169; N. L. Rosi, D. A. Giljohann, C. S. Thaxton, A. K. R. Lytton-Jean, M. S. Han and C. A. Mirkin, *Science*, 2006, **312**, 1027–1030.
6 B. V. Enustun and J. Turkevich, *J. Am. Chem. Soc.*, 1963, **85**, 3317–3328.
7 M. Zheng, Z. G. Li and X. Y. Huang, *Langmuir*, 2004, **20**, 4226–4235.
8 T. A. Taton, C. A. Mirkin and R. L. Letsinger, *Science*, 2000, **289**, 1757–1760.
9 M. C. Daniel and D. Astruc, *Chem. Rev.*, 2004, **104**, 293–346.
10 A. C. Templeton, M. P. Wuelfing and R. W. Murray, *Acc. Chem. Res.*, 2000, **33**, 27–36.
11 M. J. Hostetler and R. W. Murray, *Curr. Opin. Colloid Interface Sci.*, 1997, **2**, 42–50; J. C. Love, L. A. Estroff, J. K. Kriebel, R. G. Nuzzo and G. M. Whitesides, *Chem. Rev.*, 2005, **105**, 1103–1169; R. Shenhar and V. M. Rotello, *Acc. Chem. Res.*, 2003, **36**, 549–561.
12 W. J. Parak, D. Gerion, T. Pellegrino, D. Zanchet, C. Micheel, S. C. Williams, R. Boudreau, M. A. Le Gros, C. A. Larabell and A. P. Alivisatos, *Nanotechnology*, 2003, **14**, R15.
13 A. M. Jackson, J. W. Myerson and F. Stellacci, *Nat. Mater.*, 2004, **3**, 330–336; A. M. Jackson, Y. Hu, P. J. Silva and F. Stellacci, *J. Am. Chem. Soc.*, 2006, **128**, 11135–11149.
14 J. C. Lin and W. H. Chuang, *J. Biomed. Mater. Res.*, 2000, **51**, 413–423.
15 I. Turyan and D. Mandler, *Anal. Chem.*, 1997, **69**, 894–897.
16 T. Huang and R. W. Murray, *J. Phys. Chem. B*, 2001, **105**, 12498–12502.
17 G. A. DeVries, M. Brunnbauer, Y. Hu, A. M. Jackson, B. Long, B. T. Neltner, O. Uzun, B. H. Wunsch and F. Stellacci, *Science*, 2007, **315**, 358–362.
18 F. Dmitrii and F. Rosei, *Angew. Chem., Int. Ed.*, 2007, **46**, 6006–6008.
19 M. Brust, M. Walker, D. Bethell, D. J. Schiffrin and R. Whyman, *J. Chem. Soc., Chem. Commun.*, 1994, 801–802.
20 A. Centrone, Y. Hu, A. M. Jackson, G. Zerbi and F. Stellacci, *Small*, 2007, **3**, 814–817.
21 J. Simard, C. Briggs, A. K. Boal and V. M. Rotello, *Chem. Commun.*, 2000, 1943–1944.
22 S. Sivaramakrishnan, P. J. Chia, Y. C. Yeo, L. L. Chua and P. K. H. Ho, *Nat. Mater.*, 2007, **6**, 149–155.
23 O. Rabin, J. M. Perez, J. Grimm, G. Wojtkiewicz and R. Weissleder, *Nat. Mater.*, 2006, **5**, 118–122.

